

Extracellular vesicles aid in the transfer of long-term associative memory between *Caenorhabditis*

Supplementary Information

Supplementary methods

Behavioural assay:

The learning paradigm for long-term associative memory formation in *C. elegans* was performed as previously described with minor modifications (Dahiya *et al*, 2019). The assay can be divided into two parts (training, testing), which are described below. The training paradigm is illustrated in Figure 1A.

Training

A dry heating block was maintained at 37°C, 20 µl of 10% isoamyl alcohol (IAA)/1% Diacetyl (diluted in ethanol) was placed on top of a glass cover slip and that was in turn placed on top of the heating block. A 60 mm petri plate containing *C. elegans* was inverted on the cover slip containing IAA/diacetyl placed on the heat block for two minutes. The training cycle was repeated 5 times with an inter-training interval of 10 minutes.

Testing

This phase uses chemotaxis assay to test the memory formation in all the *C. elegans* that had been trained. Trained animals were kept for 20 hours at 22°C. *C. elegans* were picked with platinum loops and allowed to crawl on unseeded Nematode Growth media (NGM) plates for about 30 seconds.

8 to 10 animals were gently transferred to the center of a 90 mm NGM agar plate (without food). 1 µl of the native chemoattractant (1% IAA/1% heptanone/0.1% diacetyl) were placed at one end of the plate as used in previous studies (Dahiya *et al.*, 2019; Zhang *et al*, 2016). Chemotaxis behaviour was observed for the next ten minutes.

To quantify the chemotaxis behaviour, the movement of *C. elegans* away or towards the chemoattractant for all the four sets of animals was considered. If the animals move up the concentration gradient of the chemoattractant, then the displacement was considered positive. However, if the animals move down the concentration gradient of the chemoattractant, then the displacement was considered negative.

Tracking movement of *C. elegans* and its analysis:

During the testing phase of the associative learning paradigm, the plate with 8-10 *C. elegans* carrying out chemotaxis was recorded using a ThorLabs 8051C-USB camera. The setup was illuminated from underneath, with the camera mounted above the plate, for a duration of 10 minutes each.

These videos were then analysed using FIJI, and an associated plugin, Trackmate (Ershov *et al*, 2022; Schindelin *et al*, 2012). The video files were pre-processed through FIJI's suite of contrast enhancement, thresholding and background subtraction tools. Subsequently, these background-subtracted images with only *C. elegans* visible were run through the Trackmate plugin to enable spot-detection and automated track assignment, using a time-series based clustering method called Kalman filtering (implemented by the TrackMate plugin as the Kalman Tracker method). Despite the high quality of background subtraction, due to collisions in paths or occasional noise, the tracks were manually double-checked and occasionally corrected, enabling this semi-automated pipeline to be robust to any perturbations in the images.

The output of TrackMate, track files and spot files (sorted post-tracking by the unique *C. elegans* identity of each spot, per experiment), provide a number of parameters including the entire distance covered by individual *C. elegans*, average speed of the animals in a chemotaxis assay and the x- and y-coordinates of every *C. elegans* at every frame of recording. This allows us to subsequently calculate, on a per-experiment basis, the displacement of a *C. elegans* from its final position with respect to the position of the chemoattractant and the average position of a *C. elegans* over the entire chemotaxis assay. This was achieved through the use of the Pandas library for Python with its suite of vectorized operations within its data frames, allowing the integration of the spot and track outputs and computations between them.

Chemotaxis index:

This is calculated by considering the distance travelled by a *C. elegans* or *C. briggsae* and its displacement with respect to IAA/diacetyl/heptanone at the end of the ten minutes of recording. Aversive learning leads to loss of attraction towards IAA/diacetyl/heptanone, and hence, lowers the chemotaxis index from naïve conditions. The formula is as follows:

$$\text{Chemotaxis index (CI)} = \frac{\text{Displacement along the chemoattractant gradient}}{\text{Total distance travelled}}$$

The process described above was also used with for testing the CI of *C. briggsae*.

Supplementary Tables:

S1 (Strains used in this study)

Strain number	Genotype	Source
BAB9000	<i>crh-1(tz2)</i> (CGC strain YT17)	From (Dahiya <i>et al.</i> , 2019), further outcrossed 3X
BAB9001	<i>daf-22 (m130)</i> (CGC strain DR476)	Outcrossed 3X
PT1194	<i>klp-6 (my8) III; him-5(e1490) V</i>	From CGC, USA
TM5848	<i>cil-7 (tm5848) I</i> (shows him phenotype)	From NBRP, Japan
PT3602	<i>cil-7 (my61[cil-7::mNG]) I; him-5(e1490) V</i>	Gift from Maureen Barr (Wang <i>et al.</i> , 2021)
BAB9002	<i>klp-6 (my8); Pklp-6::GFP::KLP-6</i> (array, IndEx 9002)	This study
AF16	<i>C. briggsae</i> G16 isolate	From CGC, USA

S2 (Primers used in this study)

Primer Id	Sequence	Primer type	mutation
YD157	TGGAAGGAGGAGGAGATGGAAA	Genotyping (external forward)	<i>crh-1(tz2)</i>
YD158	GCAGTACAGCTCTTTCAGCGTT	Genotyping (internal forward)	<i>crh-1(tz2)</i>
YD159	AATTCGGCACAACGGACTGG	Genotyping (external reverse)	<i>crh-1(tz2)</i>
NS269	CGGTTGCTCCGATAGGATGACT	Genotyping (SNP mutant forward)	<i>daf-22 (m130)</i>
NS270	CGGTTGCTCCGATAGGATGACC	Genotyping (SNP WT forward)	<i>daf-22 (m130)</i>
NS262	CCCAGTTCACCAAGGAATTCTCTC	Genotyping (SNP mutant and WT reverse)	<i>daf-22 (m130)</i>

Supplementary figure legends:

Figure S1: Track images of naïve and trained *C. elegans*

(A) Track images of WT naïve and trained *C. elegans*, each color represents an individual *C. elegans* track. The IAA spot is indicated as a dashed circle in all track images. (B) Lifecycle of *C. elegans*, showing the time point of animal transfer. (C) Violin plots indicating CI in *C. elegans* transferred at 12 hours from training after a washing step. Multiple comparisons were done using one-way ANOVA and p-values were adjusted using Dunnett's correction; "ns" indicates not significant.

Figure S2: *C. elegans* do not gain LTAM when they are exposed to heat and IAA one after the other

(A) Track images of WT naïve, naïve *C. elegans* added to an empty plate that had had trained *C. elegans* and trained *C. elegans* added to an empty plate that had had naïve animals (ie exchange of animals from naïve to trained plates). Each color represents an individual *C. elegans* track. (B) Schematic illustration of unpaired assays, where each cue is presented one after the other instead of simultaneously. (C, D) Violin plots indicating CI in animals trained in the unpaired assays; IAA followed by heat and heat followed by IAA, respectively. Statistical analysis for S2C was performed using Mann-Whitney's non-parametric U test. Statistical analysis for S2D was performed using one-way ANOVA and p-values were adjusted using Dunnett's correction, "ns" indicates not significant in all cases.

Figure S3: Illustration of AWA and AWC neurons sensing different odours

Illustration of chemosensory neuron AWC detecting IAA and heptanone and the AWA neuron detecting diacetyl.

Figure S4: Track images of *crh-1* mutant animals

Track images of *crh-1* naïve, *crh-1* trained, *crh-1* naïve transferred to an empty plate that had had WT trained *C. elegans* and *crh-1* trained animals transferred to an empty plate that had had WT trained *C. elegans*. Each color represents an individual *C. elegans* track.

Figure S5: Track images of WT and *klp-6* mutant animals

Track images of WT naïve and trained animals in the top panels, followed by track images of *klp-6* mutants naïve and trained *C. elegans* in the middle panel. The bottom panel shows track images of *klp-6* trained animals transferred to an empty plate that had had WT trained *C. elegans* and WT trained animals transferred to an empty plate that had had *klp-6* trained *C. elegans*. Each color represents an individual *C. elegans* track.

Figure S6: Structures of molecules present exclusively on WT trained plates

The chemical structures of eight of the nine molecules found only on the WT trained plates after LC-MS analyses are indicated here in the order that they appear in the list on Figure 7A lower panel. The images were downloaded from PubChem.

Figure S7: Track images of *C. elegans* treated with a cocktail of chemicals obtained in through LC-MS analyses of treating animals with heat and IAA

(A) Track images of WT naïve, WT naïve+Imazapyr, WT naïve+2M5M, WT naïve+SGCDC and WT naïve+all 3 chemicals and trained animals recorded at 3.5 hours after chemical treatment or training. The tracks indicate response of the animals to IAA. (C) WT naïve and trained animals recorded at 3.5 hours post training. (D) WT naïve and trained animals recorded at 6 hours post training.

Figure S8: *C. briggsae* does not appear to form LTAM to IAA

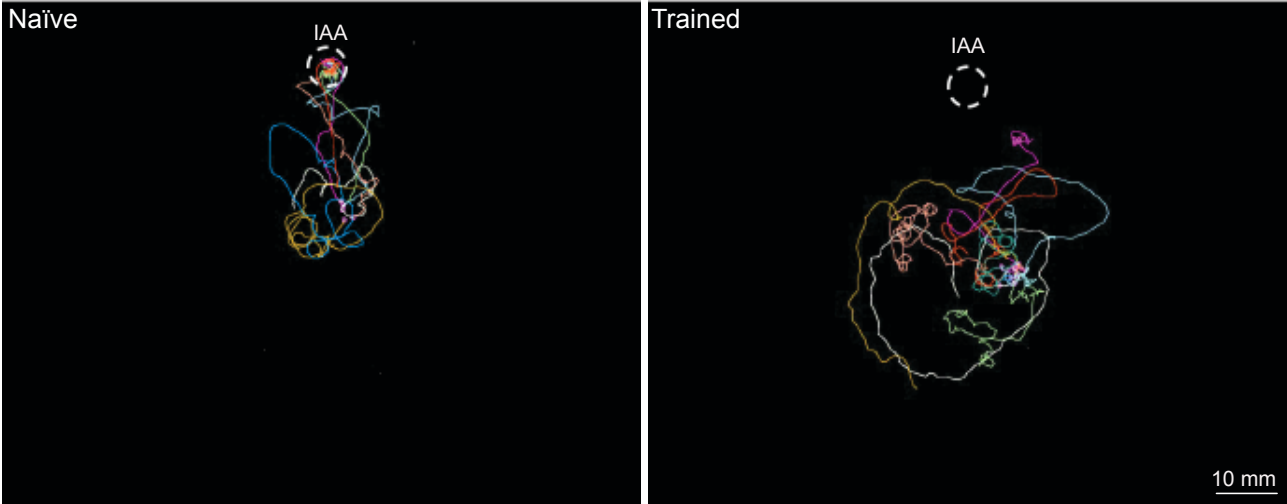
(A) Violin plots indicating CI in *C. briggsae* trained with the IAA and heat associative learning paradigm. No LTAM is seen in *C. briggsae* trained with IAA and heat. (B) Violin plots indicating CI of *C. elegans* naïve and trained, *C. briggsae* naïve, *C. briggsae* naïve transferred to an empty plate that had had trained WT *C. elegans* and *C. elegans* trained transferred to an empty plate that had had naïve *C. briggsae*. Multiple comparisons were performed using one-way ANOVA and p-values were adjusted using Dunnett's correction, "****" indicates $p < 0.0001$ and "ns" indicates not significant.

References:

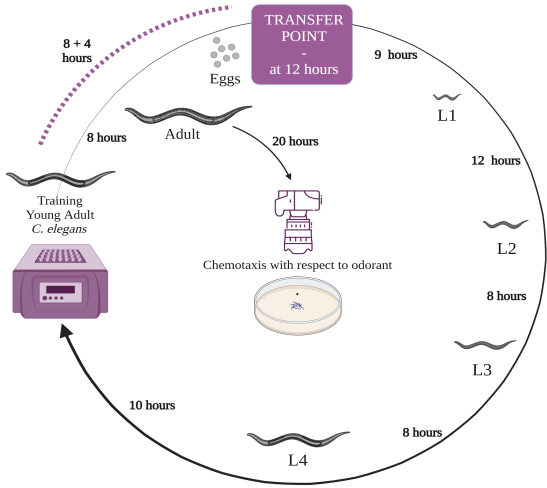
- Dahiya Y, Rose S, Thapliyal S, Bhardwaj S, Prasad M, Babu K (2019) Differential Regulation of Innate and Learned Behavior by Creb1/Crh-1 in *Caenorhabditis elegans*. *J Neurosci* 39: 7934-7946
- Ershov D, Phan MS, Pylvanainen JW, Rigaud SU, Le Blanc L, Charles-Orszag A, Conway JRW, Laine RF, Roy NH, Bonazzi D *et al* (2022) TrackMate 7: integrating state-of-the-art segmentation algorithms into tracking pipelines. *Nat Methods* 19: 829-832
- Schindelin J, Arganda-Carreras I, Frise E, Kaynig V, Longair M, Pietzsch T, Preibisch S, Rueden C, Saalfeld S, Schmid B *et al* (2012) Fiji: an open-source platform for biological-image analysis. *Nat Methods* 9: 676-682
- Wang J, Nikonorova IA, Silva M, Walsh JD, Tilton PE, Gu A, Akella JS, Barr MM (2021) Sensory cilia act as a specialized venue for regulated extracellular vesicle biogenesis and signaling. *Curr Biol* 31: 3943-3951 e3943
- Zhang C, Zhao N, Chen Y, Zhang D, Yan J, Zou W, Zhang K, Huang X (2016) The Signaling Pathway of *Caenorhabditis elegans* Mediates Chemotaxis Response to the Attractant 2-Heptanone in a Trojan Horse-like Pathogenesis. *J Biol Chem* 291: 23618-23627

Figure S1

A



B



C

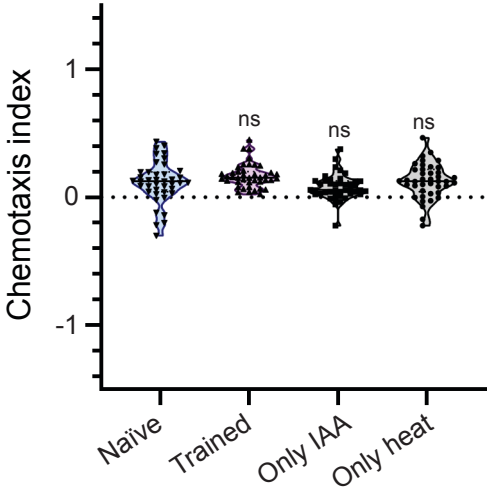
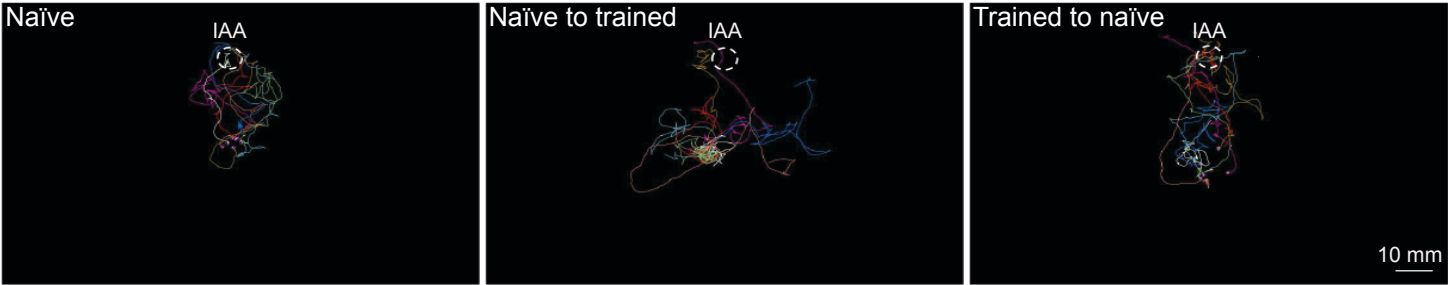


Figure S2

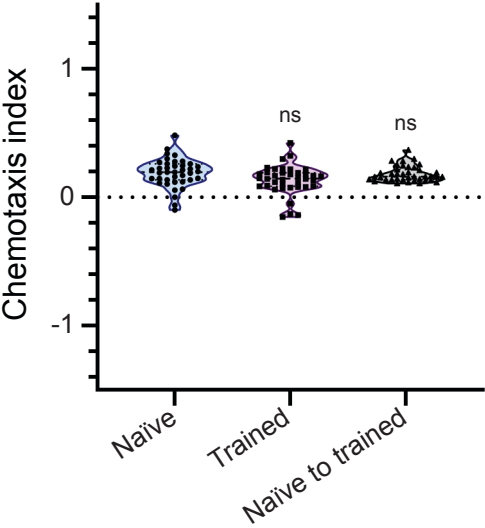
A



B



C



D

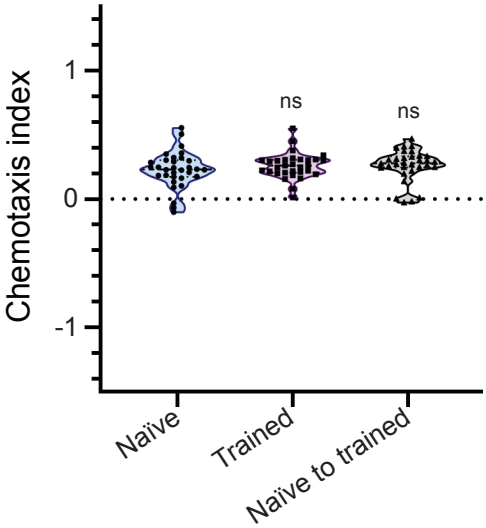


Figure S3

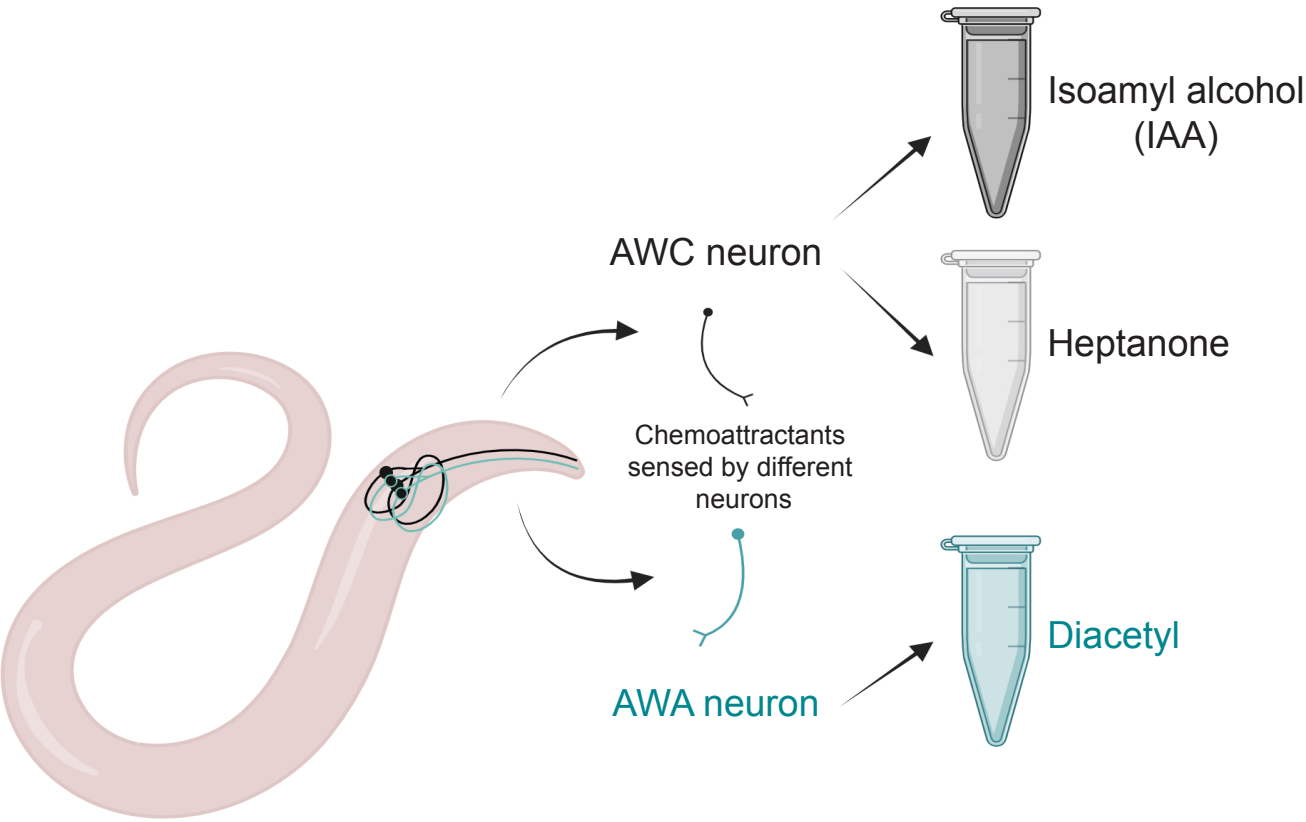


Figure S4

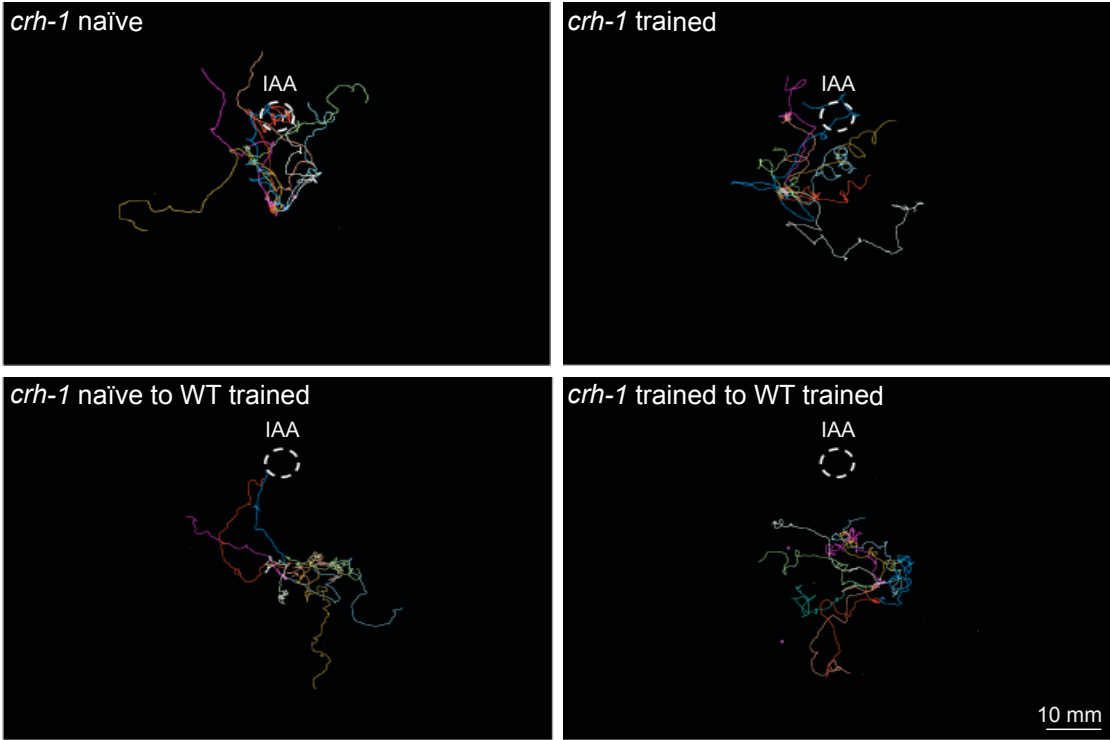


Figure S5

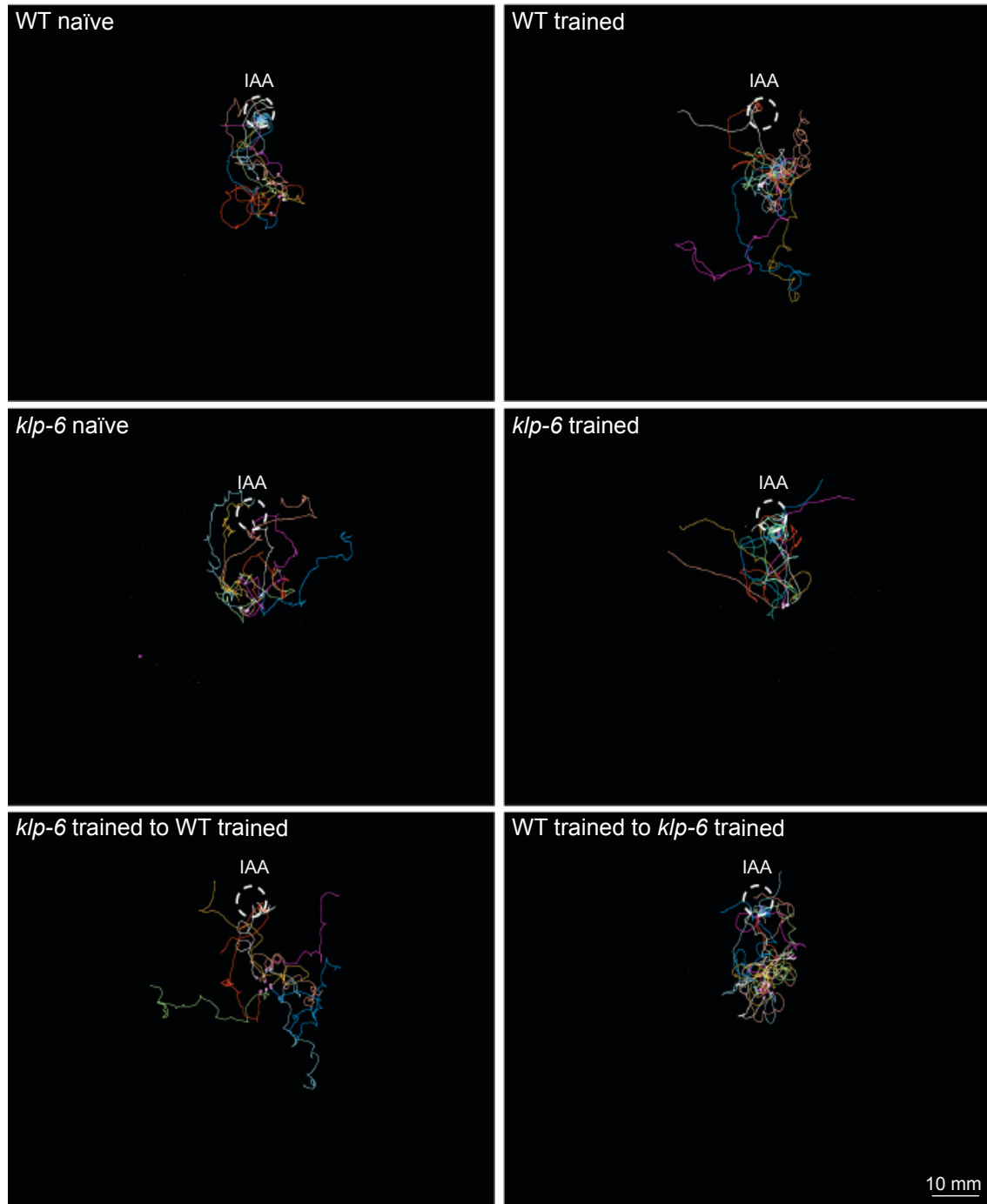
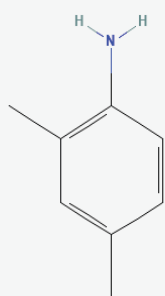
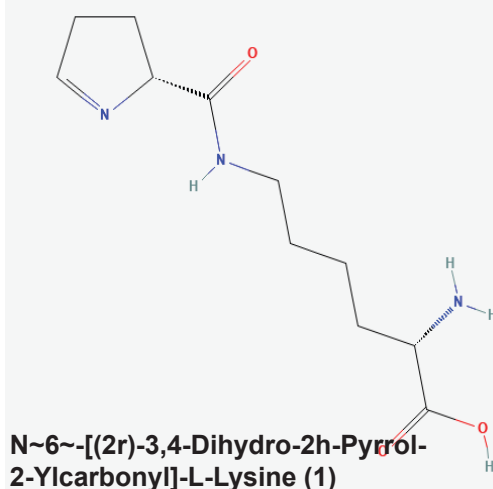


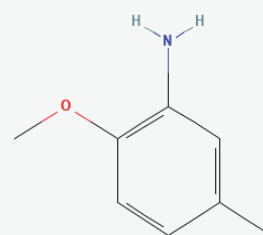
Figure S6



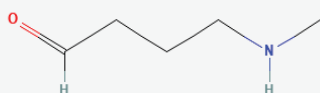
2,4-Xylidine



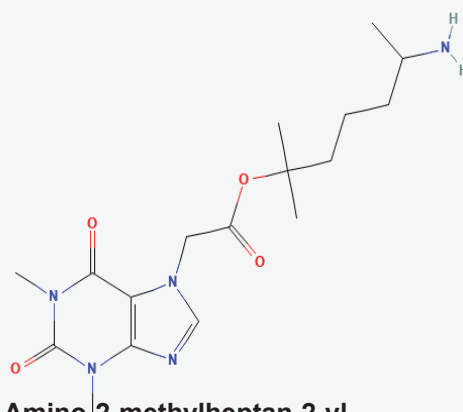
N~6~-[(2r)-3,4-Dihydro-2h-Pyrrol-2-Ylcarbonyl]-L-Lysine (1)



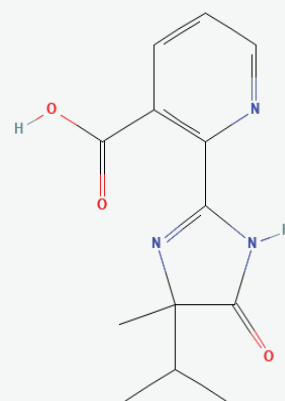
2-Methoxy 5-methylaniline (2M5M)



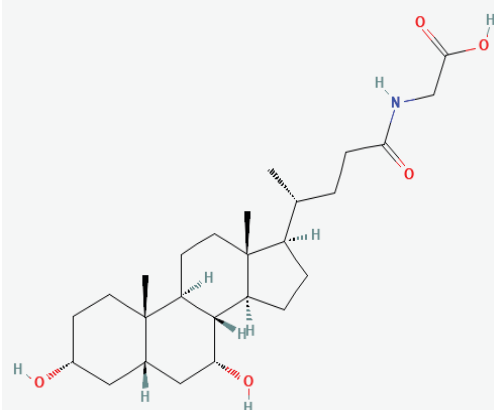
4-(Methylamino) butanal



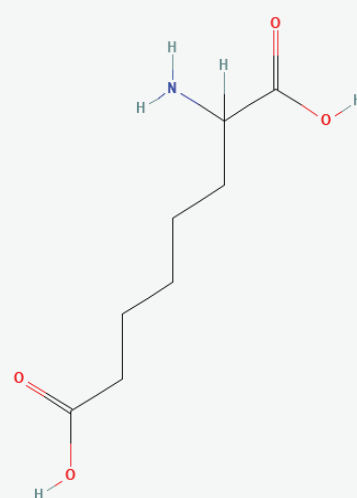
6-Amino-2-methylheptan-2-yl (1,3-dimethyl-2,6-dioxo-1,2,3,6-tetrahydro-7H-purin-7-yl)acetate



Imazapyr



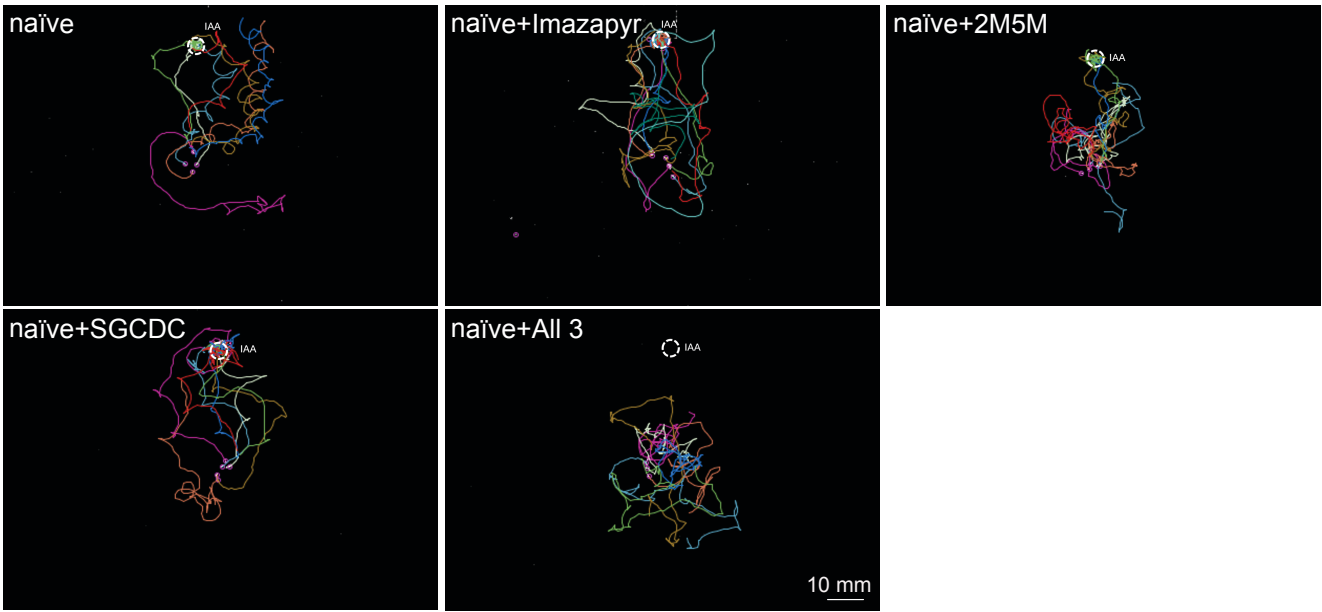
Glycochenodeoxycholic Acid (Sodium salt- SGDCDC)



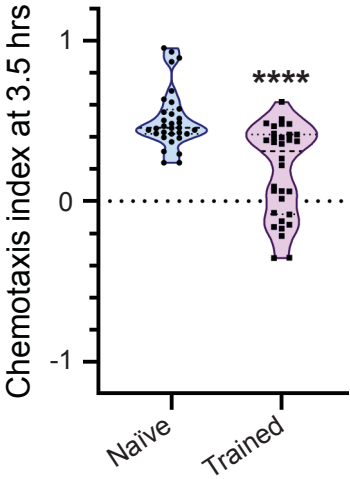
2-Aminooctanedioic acid

Figure S7

A



B



C

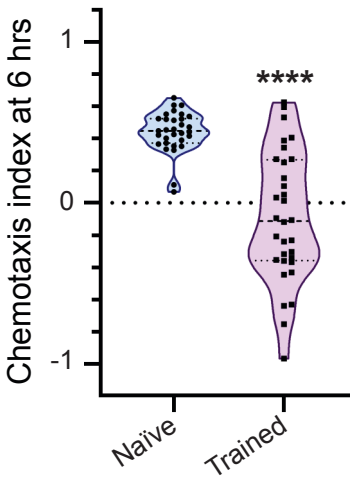
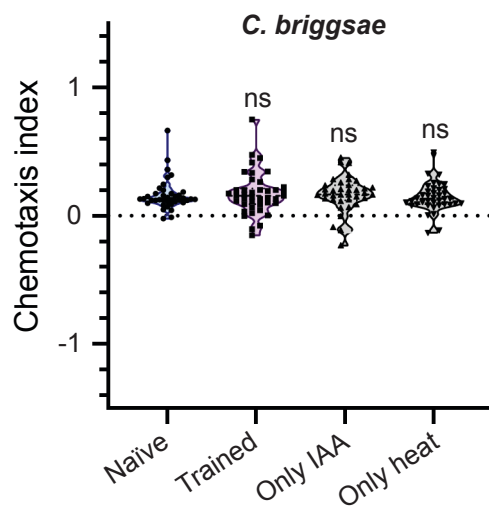


Figure S8

A



B

